ENHANCED STRUCTURE CAE SOLUTION WITH MOLDING EFFECT FOR AUTOMOTIVE PARTS

Allen Y. Peng, Wen-Hsien Yang, David C. Hsu*
CoreTech System Co., Ltd., HsinChu, Taiwan, ROC

Abstract

An increasing number of automotive parts are made of engineering plastic for its low cost and superior material properties. The traditional structure analysis for automotive injection-molded part is to perform CAE analysis based on the assumption of one or several isotropic materials. However, the material characteristic of plastic part is extremely dependent on molding process. The process-induced properties, such as fiber-induced anisotropic mechanical properties, might not be favorable to the structural requirement of final products. Besides, the mesh requirement for different analysis purposes might not be the same, either. In this paper, we integrate the CAE analysis of structure and injection molding through data-linking and mesh mapping. This approach shows the effects of mutually dependent analyses have been successfully examined in automotive injection-molded parts.

Introduction

An increasing number of automotive parts are made of engineering plastic for its low cost and superior material properties, such as fiber-reinforced plastic valve. Fiber-reinforced engineering plastic is used to substitute metal material in the manufacture of automotive products due to its superior mechanical properties and high heat distortion temperature. The traditional structure analysis for automotive part is to perform CAE analysis based on the assumption of one or several isotropic materials. However, the material characteristic of plastic part is extremely dependent on molding process. The process-induced properties, such as fiber-induced anisotropic mechanical properties, might not be favorable to the structural requirement of final products. Hence this traditional analysis procedure could neglect some molding-induced effects. Furthermore, the results of analysis could be incorrect.

The injection molding of fiber-reinforced thermoplastics is a complicated process. The reinforced composites don't possess isotropic material properties. The thermal and mechanics properties of the composite strongly depend on the fiber orientation pattern. The composite is stronger in the fiber orientation direction and weaker in the transverse direction. In this paper, we integrate the injection molding and structure analysis through an interfacing program to perform structure analysis with molding effects for fiber-reinforced plastic automotive parts.

Theory

Filling:

For the filling/packing process, the polymer melt is assumed to behave as Generalized Newtonian Fluid (GNF). Hence the non-isothermal 3D flow motion can be mathematically described by the followings.

$$\frac{\partial \rho}{\partial t} + \nabla \cdot \rho \mathbf{u} = 0 \tag{1}$$

$$\frac{\partial}{\partial t}(\rho \mathbf{u}) + \nabla \cdot (\rho \mathbf{u}\mathbf{u} - \boldsymbol{\sigma}) = \rho \mathbf{g} \tag{2}$$

$$\boldsymbol{\sigma} = -p\mathbf{I} + \eta\left(\nabla \mathbf{u} + \nabla \mathbf{u}^T\right) \tag{3}$$

$$\rho C_P\left(\frac{\partial T}{\partial t} + \mathbf{u} \cdot \nabla T\right) = \nabla(\mathbf{k}\nabla T) + \eta\dot{\gamma}^2 \tag{4}$$

where $\mathbf{u}$ is the velocity vector, T the temperature, t the time, p the pressure, σ the total stress tensor, ρ the density, η the viscosity, k the thermal conductivity, C_p the specific heat and $\dot{\gamma}$ the shear rate. The FVM due to its robustness and efficiency is employed in this study to solve the transient flow field in complex three-dimensional geometry.

Fiber orientation:

The fiber orientation state at each point in the part is represented by a 2nd-order orientation vector **A**,

$$A_{ij} = \int (p_i p_j)\varphi(p)dp \tag{5}$$

The equation of orientation change for the orientation tensor proposed by Advani and Tucker is employed for the analysis,

$$\begin{aligned}\frac{\partial A_{ij}}{\partial t} + u_k \frac{\partial A_{ij}}{\partial x_k} &= A_{ik}\Omega_{kj} - \Omega_{ik}A_{kj} + \\ &\lambda\left(A_{ik}E_{kj} + E_{ik}A_{kj} - 2A_{ijkl}E_{kl}\right) + 2C_I\dot{\gamma}\left(\delta_{ij} - 3A_{ij}\right)\end{aligned} \tag{6}$$

where C_I is the interaction coefficient with the value ranged from 10^{-2} to 10^{-3}. For the fourth-order tensor A_{ijkl}, a closure approximation is needed.

Integration approach:

This approach is to link the data between mold-filling analysis and structure analysis. The anisotropy moduli and thermal expansion coefficients of the fiber-reinforced polymer can be determined using the fiber orientation and mechanical properties of composite material. These anisotropy mechanical properties will be put into structural elements for later structure analysis. The molding-induced material properties will be taken into account in structure analysis.

Besides, the mesh requirement might be not the same for mold-filling analysis and structure analysis. The mesh of structure analysis could be focused on the area of stress concentration. However, the mesh of mold-filling analysis is stressed on the higher element resolution across the thickness direction. This approach further develops the mapping function to map the element properties from mold-filling-specified mesh to structure-specified mesh. It can correctly matches the elements and maps the material properties even though the mesh characteristics are totally different, as shown in Fig. 1.

Results and discussions

A rectangular plate of 100x50x1 mm molded with glass-fiber reinforced PET is simulated to validate the prediction of fiber orientation. Fig.2 shows the part geometry and the filling pattern. The gate is located in the center of the plate. Fig.3 displays the fiber orientation on the different cut planes. The orientation of the lines indicates the most favorable orientation direction and the color of each line represents the degree of orientation. In the vicinity of mold wall, we can see that the shearing flow tends to align the fibers along the flow. In the center cut plane, the flow is shear free and hence the fiber orientation is perpendicular to the flow direction. In Fig.4, the prediction shows the fiber alignment along the welding line. These analysis results agree well with the experimental observation.

A throttle valve made of fiber-rienforced engineering plastic is shown in Fig. 5(a). The model is meshed by 4-node tetrahedral element. Three gates are located in the same side, as shown in Fig. 5(b). The used resin is PET with 50% glass-fiber. The melt temperature is 230^{o}C, and the mold temperature is 90^{o}C. The filling time is about 2.0 second. Fig. 6(a) illustrates the predicted melt front distribution on the cavity surface. To further demonstrate how the cavity is filled, the iso-surfaces of melt front are plotted in Fig. 6(b). Fig. 7 illustrates the predicted fiber orientation on the cavity surface and inside the cavity. The orientations are extremely dependent on the filling patterns. Fig. 8 illustrates the predicted anisotropy mechanical properties. These properties will be put into later structure analysis. The temperature of whole molded part is raised 100^{o}C as the external condition to further simulate the thermal deformation of fiber-reinforced plastic valve. The constraint condition is shown in Figure 9. The commercial stress CAE – “NENastran” is employed to perform this analysis. Fig. 10 illustrates the deformation from structure analysis. Fig. 11 illustrates the von-mises stress distribution. These results show the stress distributions and deflections of the part depend heavily on the injection molding process.

Besides, a bumper with two runner designs is shown in Fig. 12(a) and Fig. 12(b). This model is a typical thin-walled part with average wall thickness of 2.9 mm. The traditional 2.5D approach is enough to obtain good analysis results. 7,331 3-node triangular plate element are used in injection molding analysis. The resin is PET with 45% glass-fiber. The fiber orientation distributions of two mold designs are illustrated in Fig. 13(a) and Fig. 13(b). Different mold designs will obtain different fiber orientation distributions. The commerical CAE – “ABAQUS” is adopted to perform the impact analysis of bumper. A mesh composed of 4-node quadrilateral plate elements and 3-node triangular plate elements is created to increase the analysis accurancy and reduce the computational loading, as shown in Fig. 14. Through the proposed mapping approach, the fiber-induced anisotropic properties is mapped correctly to this specified mesh. We assume the weight of imaginary vehicle behind the bumper is 800.0 kgw and impact a rigid column with the rate of 4.0 km/hour. The fixed constraints on bolts are also shown in Fig. 15 as red points. The period of time is 0.5 sec. The results of random orientation effects are shown in Fig. 16. Fig. 17 and Fig. 18 show the results of molding-induced orientation effects for different mold designs. Besides, to further compare the displcement histroy of sensor nodes between different mold designs, as shown in Fig. 19. All these results show the structure analysis of injection-molded plastic part depends heavily on molding conditions and mold design.

Conclusions

In this paper, we propose an integrated CAE solution for injection-molded automotive part. The results from several demonstrations show the structure analyses of fiber-reinforced plastic parts depend heavily on the molding process. Part designers are recommended to use this approach for evaluating the part design and mold design. It will be a cost-effect tool for the study of plastic part from design phase to manufacturing phase.

Acknowledgement

The authors would like to thank APIC Corp. for the partially supporting this research. The results of ABAQUS impact analysis for bumper case reported in this paper are finished under APIC Corp. assistances.

Reference

[1]. S.G. Advani and C.L. Tucker, J. Rheol., 31, 751 (1987).

[2]. "Flow-induced alignment in composite materials", ed. by T.D. Papathansiou and D.C. Guell, Cambridge (1997).

[3]. W.H.Yang, David C. Hsu, Venny Yang and R.Y.Chang, "Computer simulation of 3D short fiber orientation in injection molding", 470, ANTEC 2003, Nashville(2003)

[4]. Allen Peng, Yorker Chang, Anthony Yang, Venny Yang and F.C.Chuang, "3D fiber orientation and warpage analysis of injection-molded throttle valve", 3rd Automotive Composite Conference, Detroit(2003)

[5]. CoreTech System internal reports

Key Words

Enhance structure analysis, injection molded automotive part, Integration solution

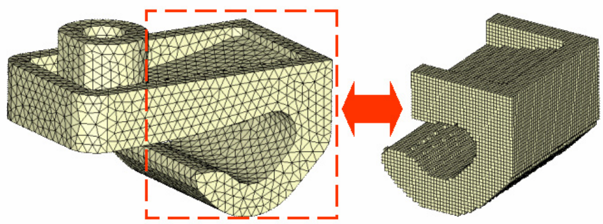

Figure 1. Map element properties between different meshes

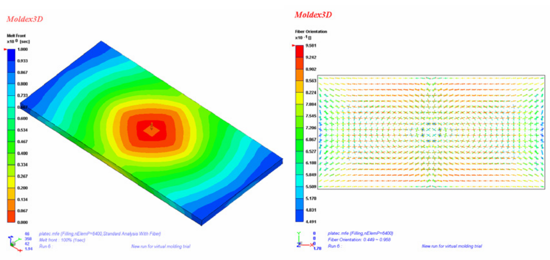

(a) Melt front (b) Fiber orientation

Figure 2. Filling results of center-gate plate

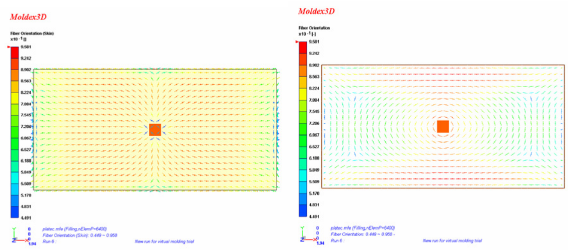

(a) On the wall (b) In the center cut plane

Figure 3. Fiber orientations distribution of center-gate plate

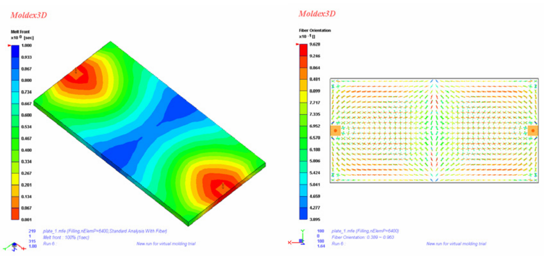

(a) Melt front (b) Fiber orientation

Figure 4. Filling results of side-gate plate

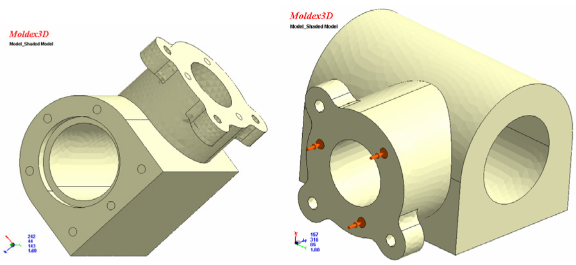

Figure 5. Throttle valve model with 3 gates

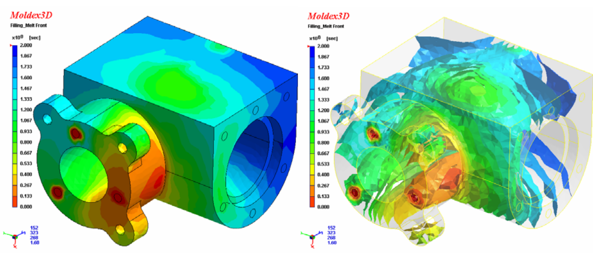

(a) Surface (b) Interior

Figure 6. Predicted melt front distribution

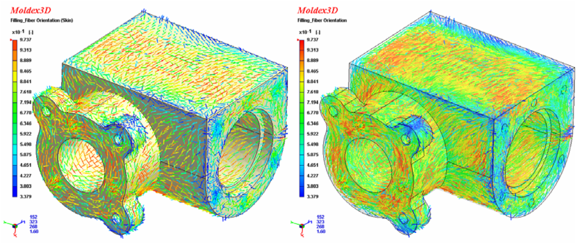

(a) Surface (b) Interior

Figure 7. Predicted fiber orientation distribution

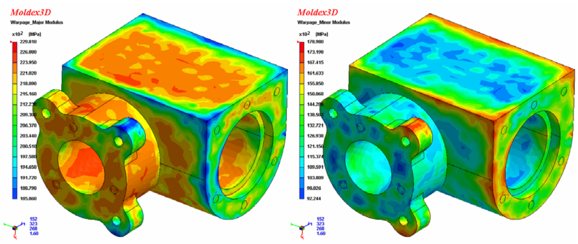

(a) Major modulus (b) Minor modulus

Figure 8. Predicted anisotropy mechanical modulus

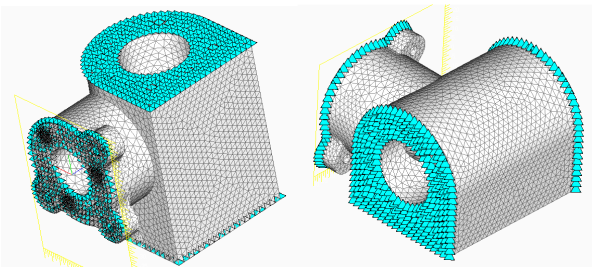

Figure 9. Constraint set for thermal stress analysis

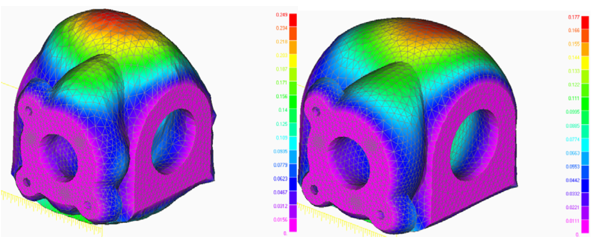

(a) (b)

Figure 10. Deformation (a) simulation with fiber orientation effects (b) simulation with random orientation effects

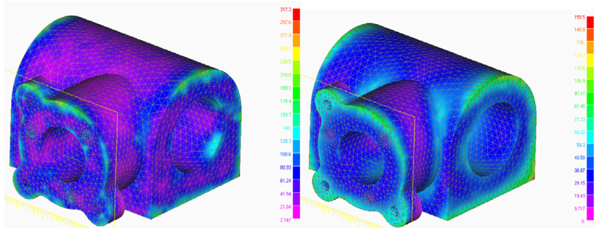

(a) (b)

Figure 11. Von-mises stress (a) simulation with fiber orientation effects (b) simulation with random orientation effects

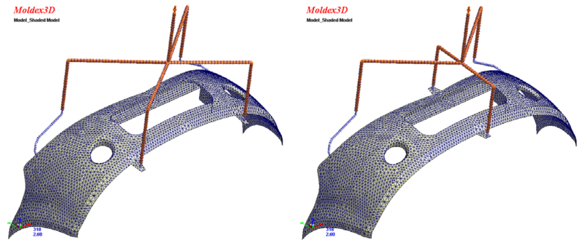

(a) Mold design 1 (b) Mold design 2

Figure 12. Bumper models with two mold designs

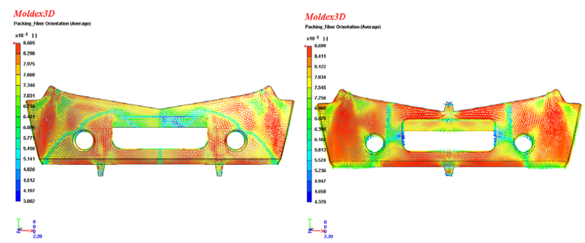

(a) Mold design 1 (b) Mold design 2

Figure 13. Average fiber orientation distributions

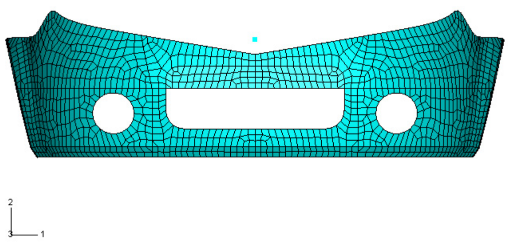

Figure 14. Specified mesh for impact analysis

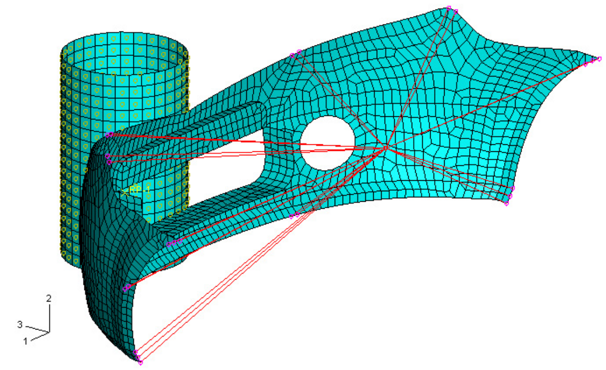

Figure 15. Models and constraints for impact analysis

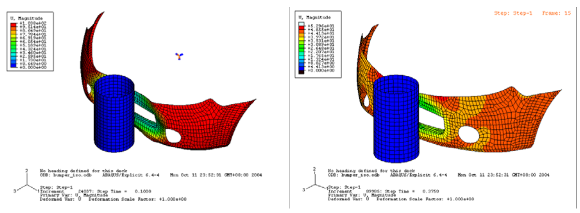

(a) 0.100 sec (b) 0.375 sec

Figure 16. Deflection of random orientation effects

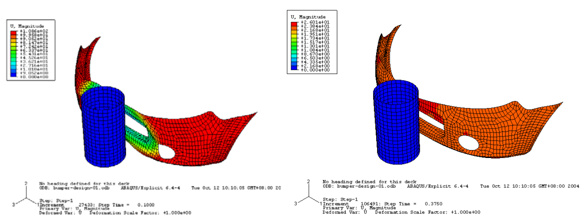

(a) 0.100 sec (b) 0.3.75 sec

Figure 17. Deflection of mold design 1

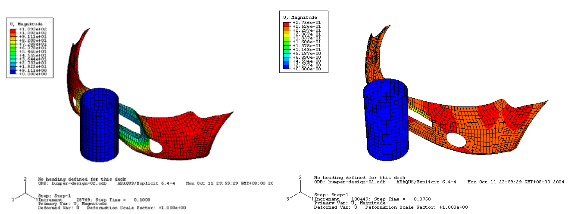

(a) 0.100 sec (b) 0.375 sec

Figure 18. Deflection of mold design 2

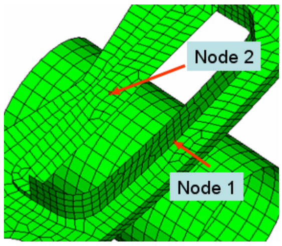

(a) Locations of sensor nodes

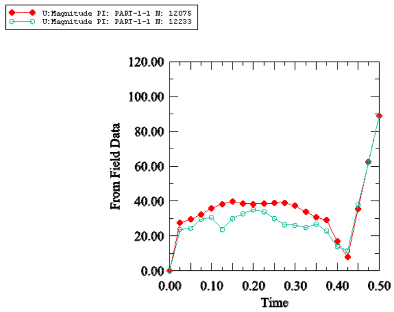

(b) Random orientation effect

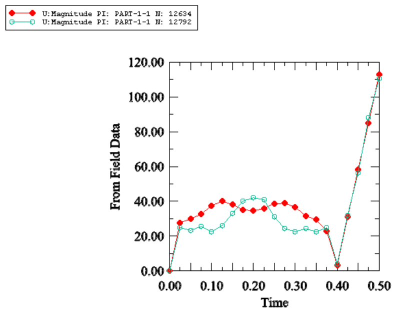

(c) Mold design 1

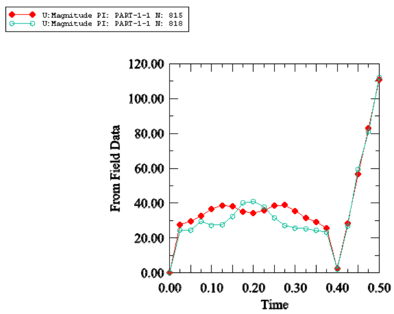

(d) Mold design 2

Figure 19. Displacement histories of sensor nodes (node 1: red line, node 2: light blue line)